Faraday Discussions

Accepted Manuscript

This manuscript will be presented and discussed at a forthcoming Faraday Discussion meeting. All delegates can contribute to the discussion which will be included in the final volume.

Register now to attend! Full details of all upcoming meetings: http://rsc.li/fd-upcoming-meetings

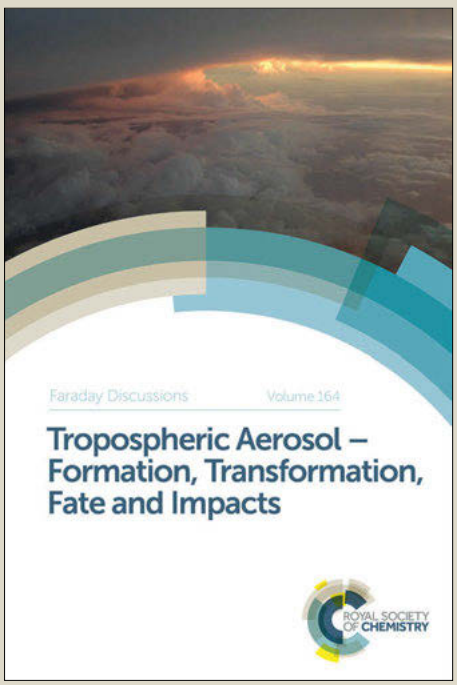

This is an *Accepted Manuscript*, which has been through the Royal Society of Chemistry peer review process and has been accepted for publication.

Accepted Manuscripts are published online shortly after acceptance, before technical editing, formatting and proof reading. Using this free service, authors can make their results available to the community, in citable form, before we publish the edited article. We will replace this *Accepted Manuscript* with the edited and formatted *Advance Article* as soon as it is available.

You can find more information about *Accepted Manuscripts* in the Information for Authors.

Please note that technical editing may introduce minor changes to the text and/or graphics, which may alter content. The journal's standard Terms & Conditions and the Ethical guidelines still apply. In no event shall the Royal Society of Chemistry be held responsible for any errors or omissions in this *Accepted Manuscript* or any consequences arising from the use of any information it contains.

ROYAL SOCIETY OF CHEMISTRY

www.rsc.org/faraday_d

Royal Society of Chemistry

Guidelines to Referees (research works)

***Faraday Discussions*—www.rsc.org/faraday_d**

For a research work to be acceptable in Faraday Discussions it **must contain new and unpublished research work** which makes a significant contribution within the scope—all aspects of physical chemistry, chemical physics and biophysical chemistry.

Review-type articles are NOT accepted and the paper must not contain more review material than is necessary to set the context for the novel work.

A Discussion paper differs from a typical research paper only in that a degree of latitude is allowed concerning inclusion of remarks or questions which may stimulate interesting scientific discussion.

A Faraday Discussion paper should be between 5,000 and 8,000 words of text plus tables and figures.

General Guidance

When preparing your report, please:

- comment on the originality, importance, impact and scientific reliability of the work;
- state unequivocally whether you would like to see the paper accepted or rejected and give detailed comments (with references, as appropriate) that will both help the Editor to make a decision on the paper and the authors to improve it;
- do not make comments about the manuscript or authors which may cause offence.

For confidentiality reasons, please:

- treat the work and the report you prepare as confidential; the work may not be retained (in any form), disclosed, used or cited prior to publication; if you need to consult colleagues to help with the review, please inform them that the manuscript is confidential, and inform the Editor;
- do not communicate directly with authors; *NB* your anonymity as a referee will be strictly preserved from the authors.

Please inform the Editor if:

- there is a conflict of interest;
- there is a significant part of the work which you are not able to referee with confidence;
- if the work, or a significant part of the work, has previously been published, including online publication (*e.g.* on a preprint server/open access server);
- you believe the work, or a significant part of the work, is currently submitted elsewhere;
- the work represents part of an unduly fragmented investigation.

When submitting your report, please:

- provide your report rapidly and within the specified deadline, or inform the Editor immediately if you cannot do so;
- submit your report at www.rsc.org/referees.

For further details, see the RSC's Refereeing Procedure and Policy — www.rsc.org/pdf/authrefs/ref.pdf

Journal Name

RSCPublishing

ARTICLE

Solvation Dynamics Monitored by Combined X-Ray Spectroscopies and Scattering: Photoinduced Spin Transition in aqueous $[Fe(bpy)_3]^{2+}$

Cite this: DOI: 10.1039/xoxxoooooox

Received ooth January 2012,
Accepted ooth January 2012

DOI: 10.1039/xoxxoooooox

www.rsc.org/

C. Bressler [a], W. Gawelda [a], A. Galler [a], M. M. Nielsen [b], V. Sundström [c], G. Doumy [d], A. M. March [d], S. H. Southworth [d], L. Young [d], G. Vankó [e]

We have studied the photoinduced low spin (LS) to high spin (HS) conversion of aqueous $Fe(bpy)_3$ with pulse-limited time resolution. In a combined setup permitting simultaneous x-ray diffuse scattering (XDS) and spectroscopic measurements at a MHz repetition rate we have unraveled the interplay between intramolecular dynamics and the intermolecular caging solvent response with 100 ps time resolution. On this time scale the ultrafast spin transition including intramolecular geometric structure changes as well as the concommittant bulk solvent heating process due to energy dissipation from the excited HS molecule are long completed. The heating is nevertheless observed to further increase due to the excess energy between HS and LS states released on a subnanosecond time scale. The analysis of the spectroscopic data allows precise determination of the excited population which efficiently reduces the number of free parameters in the XDS analysis, and both combined permit extraction of information about the structural dynamics of the first solvation shell.

A Introduction

Solvation dynamics of a photoexcited molecule concerns the interactions between the molecule and its bath, i.e., its nearest neighbor solvent molecules. This interplay manifests itself already in steady state studies by the observed Stokes shift between the absorption and emission energies of the solute [1,2], which reflect the rearrangement of the caging solvent around the excited solute. Quantum chemical calculations have meanwhile advanced and now permit simulating the dynamic response inside a box containing the excited molecule itself and a certain number of solvent molecules [3-5]. In this report we extend the experimental tools conventionally used into the x-ray domain, and apply these to a potentially functional spin transition system, aqueous iron(II) tris(bipyridine), $[Fe(bpy)_3]^{2+}$. It dynamically switches between a low spin (LS) ground to a high spin (HS) excited state upon visible light illumination, starting with a metal to ligand charge transfer (MLCT) process, followed by an ultrafast electron back transfer within 130 fs, eventually generating the spin flip to the HS state [6-8]. The bpy ligands are expected to effectively shield the central metal atom from the solvation shell, so that it appears impossible to extract any information on the solvation dynamics following the ultrafast LS-HS conversion in agreement with the optical-only results in Ref. 8. In order to address this property with structural tools we have designed an ultrafast laser-pump/x-ray probe experiment, where the probe exploits complementary structural tools to simultaneously reveal different details of the ongoing process.

A few years ago, we have implemented time-resolved x-ray emission spectroscopy at synchrotron sources using a 1 kHz amplified laser system [9], and subsequent MHz pump-probe XES studies permitted an accurate analysis of the transient XES and permitted us to extend the tools towards 1s-3p resonant XES studies [10]. Recently, we have extended time-resolved x-ray absorption spectroscopy (XAS) tools to include both x-ray emission spectroscopy (XES) and x-ray diffuse scattering (XDS) at the MHz repetition rates generated at x-ray storage rings [11]. In this contribution we extend XAS to the femtosecond time domain explored with x-ray free electron lasers (XFELs) and link this to the ps studies at storage rings, including the extraction of information content available from these simultaneously recorded x-ray emission spectra and the x-ray diffuse scattering patterns. The combination of these tools allow to acquire a complementary glimpse into the guest-host interactions.

B Experimental Approach

The picosecond experiments were assembled and conducted at beamline 7ID of the Advanced Photon Source. The setup for time-resolved x-ray absorption experiments in fluorescence detection mode at MHz repetition rates were already described in great detail [11,12]. Briefly, in the present experiments, we upgraded the standard x-ray absorption spectroscopy (XAS) equipment in total fluorescence mode by including new x-ray probing tools, which permit simultaneous x-ray emission spectroscopy (XES) and x-ray diffuse scattering (XDS)

measurements at energies above the absorption edge of the selected atom of interest (here: for Fe well above 7.1 keV).
For this purpose a secondary x-ray spectrometer in Johann configuration utilizing a spherically bent (radius: 1 m) Si(531) crystal was mounted orthogonally sideways from the incident x-ray beam to suppress the background from scattered light impinging on the crystal and its mount [10]. Just a few centimeters downstream behind the sample a 100k Pilatus detector collected elastically scattered light in forward direction in single-photon counting mode. The exciting laser beam was tuned to the MLCT absorption band of $[Fe(bpy)_3]^{2+}$ (λ = 532 nm) with adjustable frequencies tailored to the bunch filling patterns of the APS storage ring. The results below utilized the hybrid single-bunch repetition rate of 0.136 MHz, but also higher frequencies matching the 24-bunch filling pattern (6.52 MHz), with the laser tuned one half of this repetition rate (3.26 MHz) to permit laser-on and laser-off measurements in a successive fashion. With such a strategy we successfully eliminated all electronic noise contributions to the recorded signals occurring on frequencies below 1 MHz (and the majority of noise contributions occur at frequencies below one 1 kHz) [13]. This combined approach allows us to unravel different contributions in the dynamic processes of the ongoing physicochemical transformations.
In a first attempt to enter the fs time domain we exploited the LCLS for XAFS studies on the same molecule [14], which we later upgraded to allow the same combined XES and XDS measurements. Below we show the femtosecond XAFS time delay scans and our attempts to descend below the 300 fs time scale. These measurements confirm and extend our previous measurements exploiting time-sliced femtosecond x-ray pulses from the Swiss Light Source [15].
In the following we demonstrate the capabilities of x-ray absorption spectroscopy, which will serve as dearly needed input for the simultaneously applied XES and XDS tools. This approach nicely demonstrates the added value, when combining different x-ray techniques into one single experiment, as well as the additional insight from combining ps and fs results.

C X-Ray Absorption Spectroscopy: from picosecond to femtosecond time scales

Time-resolved x-ray absorption near edge structure (XANES) spectroscopy relies on detecting photoinduced modulations of the absorption cross section as a function of energy near a core shell absorption edge [16]. The absorption is dependent on both the local atomic configuration as well as on the electronic configuration, thus providing information on unoccupied electronic states and the oxidation state of the absorbing atom, and (to a lesser content) the local molecular structure (e.g., the molecular symmetry, bond angles). The XANES can be measured either in transmission mode or via total fluorescence yield, but fluorescence yield is more suitable for rather dilute samples with concentrations below around 50 mM.
In a time-resolved x-ray absorption experiment, one usually measures the transient absorption changes ΔA due to the exciting laser pulse, which generates - here for a two-level system (see Ref. 17 for the general case) - a signal of the type

$$\Delta A(t) = f(t)\,(A_{exc} - A_{gr}) \qquad (1)$$

with A_{gr} being the static (ground state) absorption, A_{exc} the excited state absorption spectrum, and $f(t)$ being the fractional excited state population, which changes as a function of time delay between the laser excitation and x-ray probe pulses. Usually there are two unknowns, namely A_{exc} and f, of which the former is the desired new result, and the latter needs to be determined separately (in a separate measurement). In some cases one can determine both unknowns using prior chemical knowledge about the excited state properties [18].

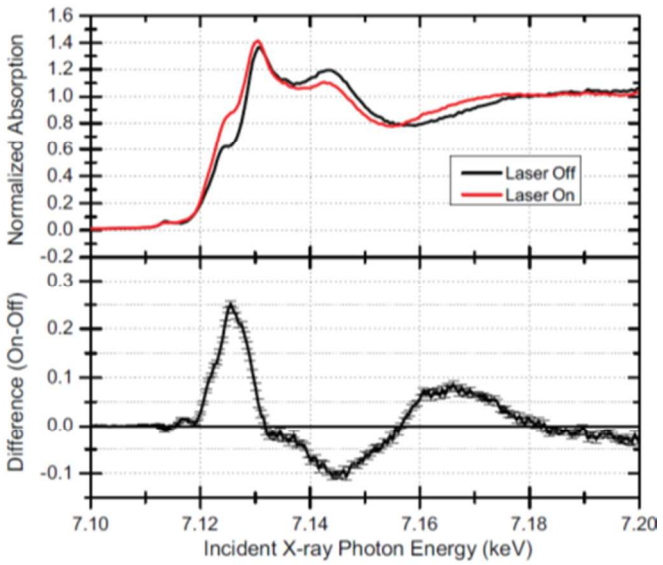

Figure 1: Time-resolved XANES of photoexcited aqueous $Fe(bpy)_3$ together with the static spectrum; below the recorded transient XANES after 100 ps (f = 0.4) [11]. Sample concentration was 20 mM, and laser excitation repetition rate was one half of the x-ray acquisition rate of 0.136 MHz.

For the present study we recorded first the TR-XANES, as shown in Fig. 1. This serves to check the overlap conditions on the sample, before switching to the combined XES/XDS experiment. To record its ultrafast temporal behavior in a fs XANES experiment exploiting XFEL radiation [14] the maximum of the transient feature was chosen [15,19,20]. XFEL experiments in general are subject to the jitter between the x-ray pulses from a linac-based SASE source and the (independent) femtosecond laser system located a kilometer downstream at the experiment. Although both light sources have been synchronized there remains an uncertainty between the relative arrival time of the x-ray pulses. When averaging successive shots to acquire sufficient signal-to-noise (S/N) for the measurement, the temporal features of the averaged signal become broadened around the nominal time delay, and this broadening leads to an instrument response function on the order of a few hundred femtoseconds. Since the studies presented here were performed prior to the implementation of single shot timing tools [21,22], the overall time resolution remained around 200-300 fs.
Figure 2 shows the analysis of the time delay data, and the black line displays the average value derived, while the false color image displays the individual data points contributing to the averaged signal. Fig. 2a shows the raw data without any time sorting treatment, while Fig. 2b displays the data after applying a rough time sorting using time arrival information

given by the so-called phase cavity, which characterizes the relative arrival time of each electron bunch [23]. This information allows us to re-sort the recorded data according to this arrival time information and the false color image in Fig. 2b shows the result of this procedure on the data in Fig. 2a. The (vertically) averaged solid black line displays hereby the same shape and rise time as for the unsorted data in Fig. 2a (around 300 fs), but one can observe a more sharper rise on the order of 150 fs in the 2D data in the same figure 2b. From this analysis we can conclude that more information can be extracted from such measurements, and exploiting a time-sorting tool in the hard x-ray domain promises to reveal higher resolved dynamic processes in the future.

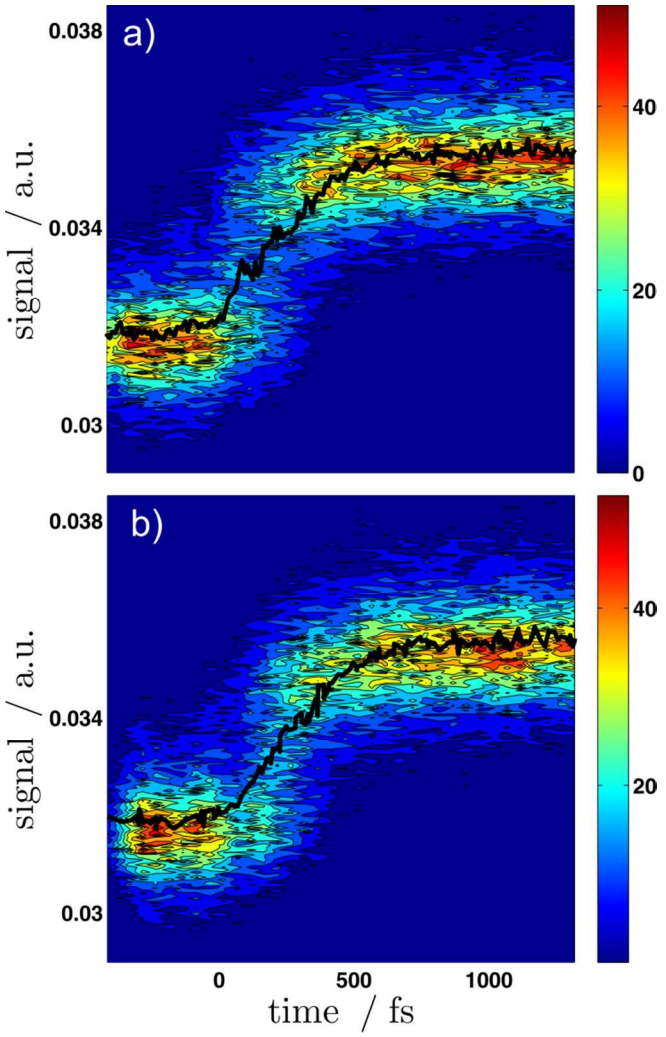

Figure 2: Femtosecond time trace of the maximum XANES transient (near 7.125 keV, see Fig. 1) recorded at an x-ray free electron (XFEL) source [14]. The dark traces in the upper and lower figures correspond to the averaged signal after 240 pump-probe shots, and the underlying false-color image shows the actual distribution of individual pump-probe shots. The upper image shows the raw recorded data, while the lower figure was generated from the data in the upper after time-sorting each shot following changes in the phase cavity timing, which delivers the steeper rise in the 2D data display than the vertically averaged values (black trace).

D Combined X-Ray Emission Spectroscopy and X-Ray Diffuse Scattering

In a setup with a MHz excitation laser we have used synchrotron radiation to study both the internal molecular processes and the involved guest-host interactions [11]. We focus hereby on the information extracted from the x-ray diffuse scattering patterns, using both XANES and XES recordings as prior input. Fig. 3a shows selected radially integrated transient XDS patterns at selected time delays covering the lifetime of the photoexcited solute. The analysis scheme is described elsewhere [11,24-26], and it relies on the identification of the major contributions to the transient XDS resulting from [11] i) the HS population, ii) the overall deposited heat into the bulk sample, but we had to also include iii) a density *increase* to achieve adequate agreement with the data at all times within the subpicosecond lifetime of the solute (Fig. 3).

Such a density increase has never before been observed in subnanosecond XDS data for molecular systems in solution, and this hints towards a special case for aqueous $Fe(bpy)_3$: in a theoretical DFT MD simulation of the LS and HS molecules embedded in a cage of water molecules Daku and Hauser determined a dramatic change of the cage structure surrounding the HS $[Fe(bpy)_3]^{2+}$ molecule [3]. They determined – on average – an expulsion of two caging water molecules into the bulk solvent, and these may be the cause of the observed density increase in the bulk solvent. In order to underline this interpretation, we have thoroughly analyzed the weights of each contribution, and linked these to our simultaneous findings via XES, and our prior findings to the XANES data. The result of this treatment is shown in Fig. 4. Fig. 4a shows the initially recorded XANES transient feature at 7.125 keV as a function of time delay nicely showing the cross correlated rise (100 ps) and the 0.6 ns exponential decay of the excited state molecules.

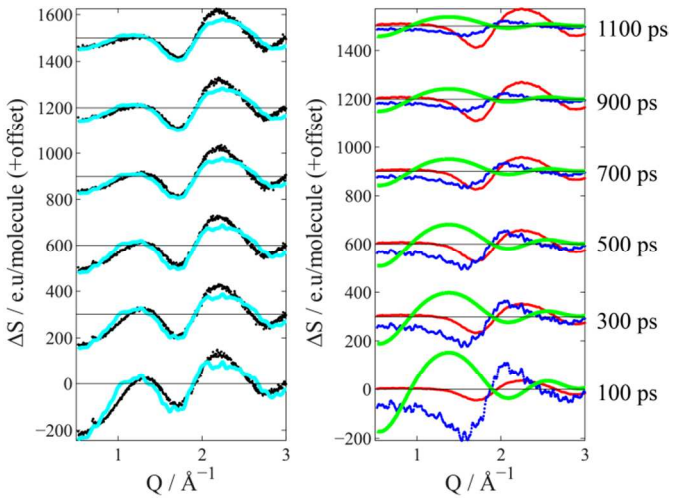

Figure 3: Transient X-ray diffuse scattering (XDS) patterns after selected time delays (indicated on the far right) of photoexcited aqueous $[Fe(bpy)_3]^{2+}$ extracted from the 2D recorded images after radial integration. The best fit curves (cyan) to the data (black) on the left were a linear superposition of the three principal transient components shown on the right: HS population (green), Bulk sample heat (red) and density increase (blue).

After moving the x-ray energy to a higher energy above the K edge (here: 7.5 keV) both XES and XDS signals were recorded simultaneously. Fig. 4a shows the time dependence of the transient XES signal together with the previously recorded XANES. One observes a slight time zero shift between both measurements, mostly owed to altered experimental synchronization conditions between both independent measurements. But more importantly, the XES decay displays the exact same time constant as measured for XANES confirming the observation of the same reaction, but also confirming the identical experimental conditions including laser fluence. Next we use the XES transient curve to fit both time zero and the instrument response function (IRF), which will flow into the XDS analysis as constant input.

The XDS contributions due to population, heat, and bulk density are displayed in Fig. 4b and fitted with a Gaussian-convoluted exponential decay function. Hereby all parameters were locked apart from their amplitudes. Thus the fit curves in Fig. 4b were extracted with constant IRF, time zero, and exponential decay constant (= locked to the previously derived values from the simultaneously recorded XES signal).

The agreement with XDS extracted population is excellent, and the heat curve shows next to an IRF broadened rise a further rise with the 0.6 ns lifetime. This can be rationalized by the energy deposited in the sample: Excitation with a 2.3 eV (532 nm) photon excites the system into its MLCT manifold, from which it relaxes well within the 100 ps IRF time into the cooled HS state, which lies about 0.6 eV above the ground state. This delivers the prompt heat signal rise within the 100 ps cross correlation time. Later, with a 0.6 ns time constant, it relaxes back into the ground state and delivers an additional heat contribution (0.6 eV per molecule into the bulk solvent), which accordingly rises exponentially with the HS lifetime (Fig. 4b, red curves). Locking even the amplitude contributions in the IRF and the exponential associated rise to the energetics given by the exciting photon energy and the intramolecular potential energies yield the dashed red curve in Fig. 4b, in close agreement to the solid curve fitted with free amplitudes. Also the quantitative values extracted from the excited state population correspond nicely to the energy deposited into the bulk slab of sample.

The density signal (blue curve in Fig. 4b) also exhibits a similar behavior as the HS population curve (green curve in Fig. 4b) and – given the DFT results in Ref. 3 – can be readily explained by the expulsion of two water molecules into the otherwise – at least on a subnanosecond time scale – incompressible liquid. This leads to – on average – a relative increase of the bulk water density (at least in the vicinity around the HS molecule) by about 5 x 10^{-4}, which is nice agreement with an estimated value of 2 water molecules x HS concentration (8 mM, or f = 40 % in a 20 mM aqueous $[Fe(bpy)_3]^{2+}$ sample). The fit curve itself does not deliver full agreement (the blue data points appear higher in amplitude than the blue fit curve), but it does display the trend of a density increase, which decays with the HS molecular lifetime, supporting the interpretation that this effect is controlled by intramolecular effects (here: the expulsion of two cage molecules into the bulk solvent). In consequence, this observation underlines the importance of guest-host interactions towards understanding molecular reactivity in the condensed phase, and further studies should aim to sharpen these tools towards a more complete understanding. It will also be interesting to see, how the density (but also the other) signals behave on the femtosecond time scale. In a future publication we treat the case of transient femtosecond XDS showing an ultrafast response of both the heat and density increase signals, which also underline the validity of the current interpretation [27].

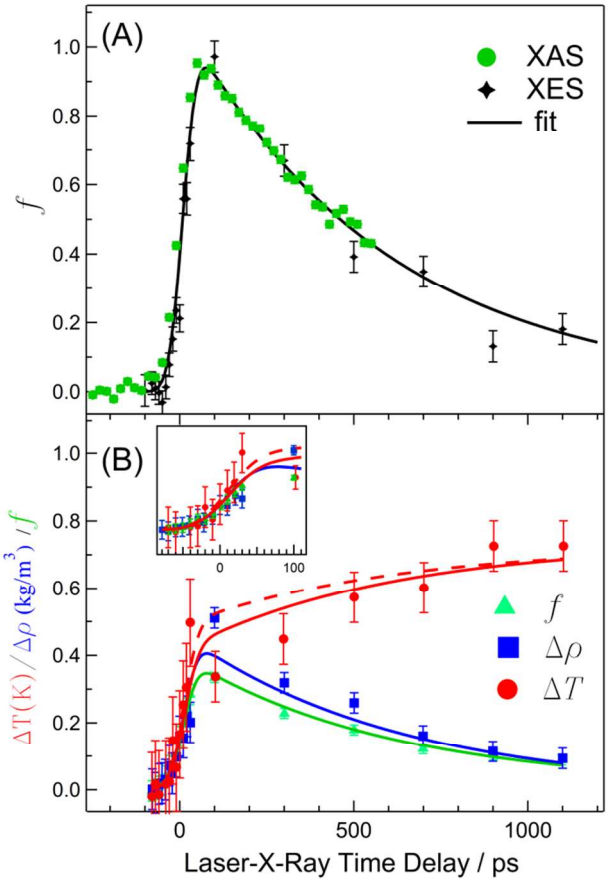

Figure 4: Analysis of the x-ray diffuse scattering patterns. A) Transient XANES signal recorded at 7.125 keV together with the XES transient recorded at 7.5 keV incident energy (and the secondary spectrometer tuned to the maximum of the $K_{\alpha 1}$ line). The XES fit curve delivers the IRF and the decay constant used in the XDS analysis in B) as fixed input (and the maximum amplitude corresponds to f = 0.4). B) Extracted weights from the XDS contributions (data points with error bars) from the superposition shown in Fig. 3 together with kinetic fits for the time traces (solid lines), for HS population (green), deposited heat (red) and density change (blue). For details see text.

E Conclusions and Outlook

The present study demonstrates the power of different, but simultaneously recorded, x-ray measurements. Time-resolved XANES and XES can extract vital electronic structural information (orbitals, spin) from the reacting species, but also deliver quantitative values for the actual fractional excited state population. Since these experiments can be reliably interpreted, they also reliably allow determining time zero and the cross correlation time, which serves as fixed input in the simultaneously recorded transient XDS patterns at different time delays. The XDS analysis can then deliver quantitative information about the global density in the bulk sample as well

as about the deposited heat therein. The XDS analysis tools can now be sharpened to permit interpreting femtosecond XDS results, and therefore this study marks a stepping stone towards a more complete understanding of chemical reactivity including dynamic guest-host interactions in the future.

Acknowledgements

We thank our collaborators and coworkers for contributing to the present work: K. Haldrup, A. Dohn, K. S. Kjaer and T. B. van Driel are acknowledged for fruitful discussions and analysis of the XDS data, E. P: Kanter; A. Bordage, H. T. Lemke, S. Canton and J. Uhlig for their help during the experiments, T. Assefa for the analysis shown in Fig. 4. This research was supported by the European XFEL, the European Research Council via contract ERC-StG-259709, by the Danish National Research Foundation's Centre for Molecular Movies, DANSCATT, and the "Lendület" (Momentum) Programme of the Hungarian Academy of Sciences. S.H.S., and L.Y. acknowledge support from the U.S. Department of Energy (DOE) Office of Science, Division of Chemical, Geological and Biological Sciences under Contract No. DE- AC02-06CH11357. A.G., W.G., and C.B. acknowledge the support of the German Research Foundation (DFG) via contract SFB925 (TP4). Portions of this work were performed at the linac coherent light source (LCLS). Use of the Advanced Photon Source, an Office of Science User Facility operated for DOE Office of Science by Argonne National Laboratory, was supported by the U.S. DOE under Contract No. DE-AC02-06CH11357.

Notes and references

[a] European XFEL, Albert-Einstein-Ring 19, 22761 Hamburg, Germany.
[b] Centre for Molecular Movies, Dept. of Physics, Technical University of Denmark, Fysikvej 307, DK-2800 Kongens Lyngby, Denmark
[c] Dept. of Chemical Physics, Lund University, Box 118, 22100 Lund, Sweden
[c] Argonne National Laboratory, 9700 South Cass Avenue, Illinois 60439, United States
[c] Wigner Research Centre for Physics, Hungarian Academy Sciences, H-1525 Budapest, Hungary

1 G. R. Fleming, M. Cho, *Annu Rev. Phys. Chem.*, 1996, **47**, 109.
2 P. Ball, *Chem. Rev*., 2008, **108**, 74.
3 L. M. L. Daku, A. Hauser, *J. Phys. Chem. Lett*., 2010, **1**, 1830.
4 T. J. Penfold, B. F. E. Curchod, I. Tavernelli, R. Abela, U. Rothlisberger, M. Chergui, *Phys.Chem.Chem.Phys*., 2012, **14**, 9444.
5 T. J. Penfold, C. J. Milne, I. Tavernelli, M. Chergui, *Pure and Appl. Chem*., 2012, **85**, 53.
6 W. Gawelda, A. Cannizzo, V.-T. Pham, F. Van Mourik, C. Bressler, M. Chergui, *J. Am. Chem. So*c., 2007, **129**, 8199-8206.
7 C. Consani, M. Prémont-Schwarz, A. El Nahhas, C. Bressler, F. Van Mourik, M. Chergui, *Angew. Chem. Int. Ed*., 2009, **48**, 7184-7187.
8 O. Bräm, F. Messina, A. M. El-Zohry, A. Cannizzo, M. Chergui, *Chem. Phys*., 2012, **393**, 51.
9 G. Vankó, P. Glatzel, V.T. Pham, R. Abela, D. Grolimund, C.N. Borca, S.L. Johnson, C.J. Milne, C. Bressler, *Angew. Chem. Int. Ed*., 2010, **49**, 34, 5910
11 K. Haldrup, G. Vankó, W. Gawelda, A. Galler, G. Doumy, A. M. March, E. P. Kanter, A. Bordage, A. Dohn, T. B. van Driel, K. S. Kjær, H. T. Lemke, S. E. Canton, J. Uhlig, V. Sundström, L. Young, S. H. Southworth, M. M. Nielsen, and C. Bressler. *J. Phys. Chem*., 2012, A **116**, 9878.
12 A. March, A. Stickrath, G. Doumy, E. P. Kanter, B. Krässig, S. H. Southworth, K. Attenkofer, C. A. Kurtz, L. X. Chen, L. Young, *Rev. Sci. Instrum*., 2011, **82**, 073110.
13 W. Gawelda, C. Bressler, M. Saes, M. Kaiser, A.N. Tarnovsky, D. Grolimund, S.L. Johnson, R. Abela, M. Chergui, *physica scripta*, 2005, **T115**, 102.
14 H. T. Lemke, C.Bressler , L.X. Chen, D. M. Fritz, K. J. Gaffney, A. Galler, W. Gawelda, K. Haldrup, R. W. Hartsock, H. Ihee, J. Kim, K. H. Kim, J. H. Lee, M. M. Nielsen, A. B. Stickrath, W. Zhang, D. Zhu, M. Cammarata, *J. Phys. Chem*., 2013, A**117**, 735.
15 Ch. Bressler, C. Milne, V.T. Pham, A. ElNahhas, R. M. van der Veen, W. Gawelda, S. Johnson, P. Beaud, D. Grolimund, C. N. Borca, G. Ingold, R. Abela, and M. Chergui, *Science*, 2009, **323**, 489.
16 C. Bressler, M. Chergui, *Chem. Rev*., 2004, **104**, 1781.
17 C. Bressler, R. Abela, M. Chergui, *Z. Krist*., 2008, **223,** 307.
18 W. Gawelda, V.-T. Pham, R. M. van der Veen, D. Grolimund, R. Abela, M. Chergui, and C. Bressler, *J. Chem. Phys*., 2009, **130**, 124520.
19 W. Gawelda, V.-T. Pham, A. El Nahhas, M. Kaiser, Y. Zaushitsyn, S.L. Johnson, D. Grolimund, R. Abela, A. Hauser, C. Bressler, M. Chergui, *AIP Conf. Proc*., 2007, **882**, 31.
20 . Gawelda, V.-T. Pham, A. El Nahhas, Y. Zaushitsyn, M. Kaiser, D. Grolimund, S.L. Johnson, R. Abela, A. Hauser, C. Bressler, M. Chergui, *Phys. Rev. Lett*., 2007, **98**, 057401.
21 M. R. Bionta, H. T. Lemke, J. P. Cryan, J. M. Glownia, C. Bostedt, M. Cammarata, J.-C. Castagna, Y. Ding, D. M. Fritz, A. R. Fry, J. Krzywinski, M. Messerschmidt, S. Schorb, M. L. Swiggers, and R. N. Coffee. *Opt. Express*, 2011, **19**, 21855.
22 M. Harmand, R. Coffee, M. R. Bionta, M. Chollet, D. French, D. Zhu, D. M. Fritz, H. T. Lemke, N. Medvedev, B. Ziaja S. Toleikis and M. Cammarata. *Nature Photonics*, 2013, **7**, 215.
23 J. M. Glownia et al., *Optics Express*, 2010, **18**, 17620.
24 M. Christensen, K. Haldrup, K. Bechgaard, R. Feidenhans'l, Q. Kong, M. Cammarata, M. L. Russo, M. Wulff, N. Harrit, M. M. Nielsen, *J. Am. Chem. Soc*., 2009, **131**, 502.
25 . Cammarata, M. Lorenc, T. Kim, J.H. Lee, Q. Y. Kong, E. Pontecorvo, M. L. Russo, G. Schiro, A. Cupane, M. Wulff, H. Ihee, *J. Chem. Phys*., 2006, **124**, 1245041-9.
26 K. Haldrup, M. Christensen and M.M. Nielsen, *Acta Cryst. A*, 2010, **66**, 261.
27 C. Bressler *et al.*, to be published (2014).